Nonlinear Fabry–Perot resonator with a silicon photonic crystal waveguide

Kazuhiro Ikeda and Yeshaiahu Fainman

Department of Electrical and Computer Engineering, University of California, San Diego, 9500 Gilman Drive, La Jolla, California 92093-0409

Received July 13, 2006; revised September 8, 2006; accepted September 8, 2006; posted September 13, 2006 (Doc. ID 72992); published November 9, 2006

We derive an equation that describes the nonlinear operation of a Fabry–Perot resonator with a large group index waveguide. Specifically, a silicon photonic crystal microcavity with two-photon-excited free carrier nonlinearity and Kerr nonlinearity is assumed. The equation clearly explains the bistability of the device and the reduction of the required pump energy for a specific nonlinear phase shift at an appropriate phase detuning from the resonance. We present a simple procedure to predict the required optical pump energy for the modulation and the resulting modulation depth by use of the equation and the device parameters.

OCIS codes: 190.1450, 190.4360, 230.5750.

Silicon photonics has become an active research area due to its compatibility with standard complimentary metal-oxide semiconductor technology, resulting in demonstration of various silicon-based devices such as modulators,[1] lasers,[2] and switches.[3] Since the nonlinear effects in silicon are very small, field localization using resonant nanostructures[3–6] is being developed to enhance the efficiency of nonlinear optical processes. Specifically, ultrahigh-quality factors that have been demonstrated in silicon photonic crystal (PhC) microcavities[7] are attractive for enhancing the efficiency of nonlinear interactions in silicon-based devices.[4] However, to our knowledge detailed analysis of resonant cavities realized with PhC lattices has not yet been sufficiently advanced. In this Letter, we introduce a simple analysis of the nonlinear phase shift in a Fabry–Perot resonator realized with a two-dimensional (2D) PhC waveguide in silicon. For given linear parameters of a resonator, we present an analytic procedure to predict the optical pump energy required to achieve nonlinear operation of a Fabry–Perot resonator with the desired modulation depth.

Consider a simple model described in the diagram in Fig. 1, where the two mirrors with amplitude reflectance r, amplitude transmittance t, and amplitude scattering loss s are placed at $z=0$ and $z=L$, respectively. We assume that the waveguide between them has material index n and corresponding group index n_g (equivalently group velocity v_g). We also assume that the refractive index n of the material changes due to the nonlinear Kerr effect, $n_2 I$, and to the Drude effect via free carrier generation by two-photon absorption (TPA), $n_d I^2$:

$$n = (n_0 - jn'_0) + n_d I^2 + (n_2 - jn'_2)I, \tag{1}$$

where n_0 and n_0' are the real and the imaginary part of the linear refractive index of the waveguide material, respectively; n_2 and n_2' are the real and imaginary part of the nonlinear refractive index due to Kerr nonlinearity, respectively. Assuming a Gaussian-shaped pump pulse with full width at half-maximum (FWHM), τ_p, and angular frequency ω_p, the value of n_d can be expressed for a time scale much shorter than the carrier lifetime as[8]

$$n_d = \frac{-e^2}{2n_0\omega_s^2 m^* \epsilon_0}\frac{\tau_p\sqrt{\pi}}{\sqrt{4\ln 2}}\frac{\beta}{2\hbar\omega_p}, \tag{2}$$

where e is the electron charge, ω_s is the angular frequency of the signal, m^* is the effective mass of electrons and holes ($=0.16m_0$, with m_0 being the mass of the electron), ϵ_0 is the vacuum permittivity, and β is the TPA coefficient. The propagation constant for the field inside the waveguide shown in Fig. 1 is given by

$$k = k_0 n_g = k_0\frac{n}{\cos\theta}, \tag{3}$$

where k_0 is the free-space wavenumber and θ is the angle between the waveguide direction and the direction of the phase velocity. The zigzag ray picture for the group index is valid for the strongly confined waveguide, where the effect of Goos–Hänchen shift can be neglected,[9] which will be the case for a 2D PhC waveguide when the small dispersion from material and vertical index guiding is neglected. Substituting Eq. (1) into Eq. (3) yields

$$k = \frac{k_0}{\cos\theta}(n_0 + n_d I^2 + n_2 I) - j\left(\frac{\alpha+\beta I}{2\cos\theta}\right) \equiv \kappa - j\mu, \tag{4}$$

where $\alpha = 2k_0 n_0'$ is the attenuation coefficient that includes losses due to single-photon absorption and waveguide loss, and $\beta = 2k_0 n_2'$ is the TPA coefficient already defined. Here, we also defined κ and μ as the real and the imaginary part of the propagation constant, respectively. A large value of n_g (or large θ) can be achieved using a PhC waveguide,[10] and we apply our theory to the PhC microcavity later. We find the intensity of the field inside the cavity, $I(z)$, normalized to the intensity of the input field, $|a|^2$:

0146-9592/06/233486-3/$15.00

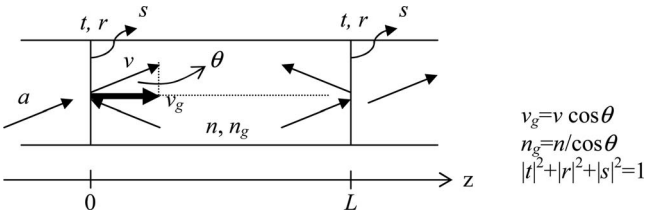

Fig. 1. Schematic diagram describing the analytic model for Fabry–Perot resonator in a large group index waveguide.

$$\frac{I(z)}{|a|^2} = \frac{e^{-2\xi(z)} + R^2 e^{-4\xi(L)} e^{2\xi(z)} + 2R\, e^{-2\xi(L)} \cos 2[\phi(L) - \phi(z)]}{1 - 2R^2 e^{-2\xi(L)} \cos 2\phi(L) + R^4 e^{-4\xi(L)}} \times (1 - S^2 - R^2), \quad (5)$$

where we assumed real values for the reflectance, $r = R$, and the scattering loss, $s = S$, and the phase $\phi(z)$ and the attenuation $\xi(z)$ are given by

$$\phi(z) = \int_0^z \kappa(z')\mathrm{d}z' = \frac{k_0 n_0 z}{\cos\theta} + \frac{k_0}{\cos\theta}\left[n_d \int_0^z I^2(z')\mathrm{d}z' + n_2 \int_0^z I(z')\mathrm{d}z' \right], \quad (6)$$

$$\xi(z) = \int_0^z \mu(z')\mathrm{d}z' = \frac{\alpha z}{2\cos\theta} + \frac{\beta}{2\cos\theta}\int_0^z I(z')\mathrm{d}z'. \quad (7)$$

Equation (5) can be solved for I together with Eqs. (6) and (7) for $\phi(z)$ and $\xi(z)$, respectively, as they both depend on I in the nonlinear regime. The resulting solution will be multivalued, indicating that the resonator will become bistable[11] when the pump has a wavelength (or phase) detuned from the resonance and the input intensity $|a|^2$ is large enough. The solutions are described graphically in Fig. 2 by plotting the left-hand side (LHS) of Eq. (5), which is a straight line with tilt $1/|a|^2$, and the right-hand side (RHS), which is the same curve as the cavity spectrum, with regard to I. If the pump wavelength is at the resonant wavelength or has a small phase detuning ϕ [if the first term of Eq. (6) at $z = L$ is zero or ϕ], then the solution is still single valued, and as the input intensity increases it increases following the resonant curve (see the circles in Fig. 2). When the pump wavelength has a large phase detuning ϕ', as the input intensity increases, the solution is at first single valued and gradually increases. However, after the straight line crosses the peak of the resonant curve of the RHS, the solution becomes triple valued, and the physical solution is the smallest (largest) point for the ascending (descending) of the pump pulse. Finally, after the crossing point of the smallest solution vanishes, the solution jumps to the largest value and again becomes single valued. If we compare the solutions with no detuning to that with a value of ϕ (see Fig. 2), the required input intensity $|a|^2$ for ϕ detuning is smaller than that for no detuning, for the same modulation depth δ and the same phase shift ϕ. Thus, with an appropriate phase detuning, the required input intensity can be significantly reduced. Solving Eq. (5), we can easily predict the optimum pump phase detuning and the required pump power for switching operation by using the material and the measured linear parameters of the device.

We first simplify integral equations (5)–(7) by removing the z dependence in I. We assume that the phase and the loss inside the cavity are independent of z as $\phi(z) = m\pi$, $\xi(z) = \frac{1}{2}\xi(L)$. With this assumption, we can use the position-independent intensity I_p, which represents the peak intensity inside the cavity with the loss at the center of the cavity, instead of $I(z)$ in Eqs. (5)–(7). Thus, we can simplify the integrals in Eqs. (6) and (7) as

$$\phi(L) = \frac{k_0 n_0 L}{\cos\theta} + \frac{k_0 n_2 L_{\mathrm{eff1}}}{\cos\theta} I_p + \frac{k_0 n_d L_{\mathrm{eff2}}}{\cos\theta} I_p^2, \quad (8)$$

$$\xi(L) = \frac{\alpha L}{2\cos\theta} + \frac{\beta}{2\cos\theta} I_p L_{\mathrm{eff1}}, \quad (9)$$

where the effective length L_{eff1} and L_{eff2} are given by $L_{\mathrm{eff1}} = \int_0^L I(z')\mathrm{d}z'/I_p$, $L_{\mathrm{eff2}} = \int_0^L I^2(z')\mathrm{d}z'/I_p^2$, $\beta = n_d = n_2 = 0$. Note that with an approximation of $e^x \sim 1 + x$ and $\cos 2x \sim 1 - 2x^2$, which is appropriate for a high-finesse and low-loss cavity mode, Eq. (5) reduces to a 6th-order algebraic equation for I_p.

Next we compare our analysis with the experimental data from Ref. 4, where linear parameters of a PhC microcavity and the nonlinear operation were measured. We use the following measured parameters for the linear regime of operation: resonant wavelength $\lambda_r = 1547.68$ nm ($= \lambda_s = \lambda_p$, the degenerate case), free spectrum range FSR $= 1568.05 - 1530.47 = 37.58$ nm, FWHM of the resonant mode of $\Delta\lambda = 0.084$ nm, waveguide loss $\alpha(\mathrm{dB}) = 1$ dB/mm,[12] cavity length $L = 4 \times 0.42 = 1.68\ \mu$m, and core area $A = 0.2 \times \sqrt{3} \times 0.42 = 0.145\ \mu\mathrm{m}^2$. We estimate the following values: (i) group index $n_g = 15.2$ from λ_r and FSR and (ii) reflectance $R = 0.9974$ from $\Delta\lambda$ and α (dB). S is set to zero. We assumed material parameters $n_0 = 3.46$, $n_2 = 0.45 \times 10^{-13}\ \mathrm{cm}^2/\mathrm{W}$, and $\beta = 0.8$ cm/GW.[13] To predict the nonlinear operation, we first calculate $n_d = -4.7 \times 10^{-31}\ \mathrm{m}^4/\mathrm{W}^2$ with $\tau_p = 7.3$ ps, which was used in the experiment in Ref. 4. Estimating the coeffi-

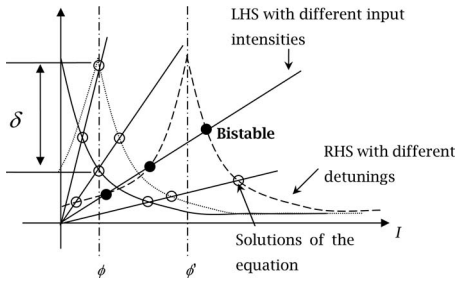

Fig. 2. Schematic plots of the LHS and RHS of Eq. (5). The circles are solutions for various input intensities and phase detunings.

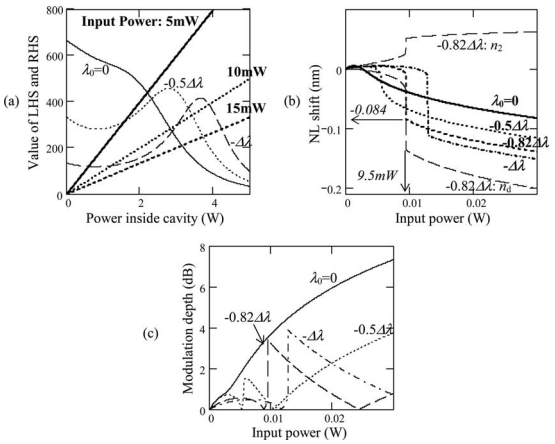

Fig. 3. Plots of the solutions of Eq. (5) for data from Ref. 4. (a) Plots of LHS and RHS of Eq. (5) with relation to power inside the cavity for various input peak powers and wavelength detunings. (b) Nonlinear phase shift and (c) modulation depth in relation to the input peak power for various wavelength detunings.

cients ξ_1 in Eqs. (8) and (9) with $L_{\text{eff1}} \sim L_{\text{eff2}} \sim L$, we use Mathcad to solve the 6th-order algebraic equation approximating Eq. (5) (see Fig. 3). Specifically, Fig. 3(a) shows plots of the LHS and RHS of Eq. (5) with different input powers and different wavelength detunings $\lambda_0 = -\phi_0 \lambda_r^2/(2\pi n_g L)$. Comparing Fig. 3(a) with Fig. 2, we can see small redshifts due to the Kerr effect at low power and resonant peak degradations due to TPA in the RHS curves. Figure 3(b) shows the wavelength shift with regard to the input peak power for different values of λ_0. For the 0.084 nm of the FWHM wavelength shift, the required input power is 9.5 mW with a detuning of $-0.82\Delta\lambda$, corresponding to $7.3\ \text{ps} \times 9.5\ \text{mW} = 69.4\ \text{fJ}$. The experimental value in Ref. 4 was 100 fJ, and the energy effectively coupled to the cavity was estimated as 10 fJ to take into account the broad spectrum of the pump pulse and the transmission bandwidth of the cavity. Consequently, our estimated analytic value is close to the experimental results, with error due to the uncertainty in the values of waveguide loss, group index, and mode volume. According to our dimensions, the volume $V = AL = 0.24\ \mu\text{m}^3$, which is three times larger than its mode volume of $0.07\ \mu\text{m}^3$ given in Ref. 4. If we use the volume of $V/3$ with $(1/3)^{2/3} A$ and $(1/3)^{1/3} L$, the required pump power is calculated as 3.3 mW, leading to pump energy of 24.1 fJ, which will be more accurate. In Fig. 3(b), the portions due to the Kerr effect (n_2) and the Drude effect (n_d) are also drawn separately for $\lambda_0 = -0.82\Delta\lambda$, which indicates that the Drude effect overcomes Kerr effect. Figure 3(c) can be used to obtain the modulation depth. Because of the significant peak degradation from TPA seen in Fig. 3(a), the reduction of the required pump power explained in Fig. 2 is not observed, and zero phase detuning is optimum in this case. The above procedure could be applied in the same way to any other cavity structure, such as a ring resonator, by using its analytic expression[14] for the internal intensity instead of that in Eq. (5).

In conclusion, we derived an equation that describes the nonlinear operation of a Fabry–Perot resonator with a large group index waveguide. Specifically, a silicon PhC microcavity with nonlinearities due to the two-photon-excited free carrier effect and the Kerr effect was assumed. The equation clearly explained the bistability of the device and the reduction of the required pump energy for a specific nonlinear phase shift or modulation depth at an appropriate phase detuning from the resonance. We presented a simple procedure to predict the required optical pump energy for the modulation and the resulting modulation depth by using the equation and the device parameters. Compared with coupled mode analysis[15] or rate equation analysis,[16] this procedure makes it straightforward to see intuitively why bistable operation happens or how phase detuning and loss due to TPA affect the bistability and the device operation.

The authors thank H.-C. Kim and U. Levy for valuable discussions and A. Krishnamoorthy and J. Cunningham at Sun Microsystems for their support and encouragement. Financial support from the National Science Foundation, the Air Force Office of Scientific Research, and the Defense Advanced Research Projects Agency is gratefully acknowledged. K. Ikeda (kazikeda@ucsd.edu) acknowledges a scholarship from the Nakajima Foundation, Japan.

References

1. A. Liu, R. Jones, L. Liao, D. Samara-Rubio, D. Rubin, O. Cohen, R. Nicolaescu, and M. Paniccia, Nature **427**, 615 (2004).
2. H. Rong, R. Jones, A. Liu, O. Cohen, D. Hak, A. Fang, and M. Paniccia, Nature **433**, 725 (2005).
3. V. R. Almeida, C. A. Barrios, R. R. Panepucci, and M. Lipson, Nature **431**, 1081 (2004).
4. T. Tanabe, M. Notomi, S. Mitsugi, A. Shinya, and E. Kuramochi, Appl. Phys. Lett. **87**, 151112 (2005).
5. W. Nakagawa and Y. Fainman, IEEE J. Quantum Electron. **10**, 478 (2004).
6. H.-C. Kim, K. Ikeda, and Y. Fainman, "Tunable transmission resonant filter and modulator with vertical gratings," submitted to J. Lightwave Technol.
7. B.-S. Song, S. Noda, T. Asano, and Y. Akahane, Nat. Mater. **4**, 207 (2005).
8. H. W. Tan, H. M. van Driel, S. L. Schweizer, R. B. Wehrspohn, and U. Gosele, Phys. Rev. B **70**, 205110 (2004).
9. H. Kogelnik and H. P. Weber, J. Opt. Soc. Am. **64**, 174 (1974).
10. M. Notomi, K. Yamada, A. Shinya, J. Takahashi, C. Takahashi, and I. Yokohama, Phys. Rev. Lett. **87**, 253902 (2001).
11. R. W. Boyd, *Nonlinear Optics* (Academic, 1992).
12. M. Notomi, A. Shinya, S. Mitsugi, E. Kuramochi, and H.-Y. Ryu, Opt. Express **12**, 1551 (2004).
13. M. Dinu, F. Quochi, and H. Garcia, Appl. Phys. Lett. **82**, 2954 (2003).
14. L. F. Stokes, M. Chodorow, and H. J. Shaw, Opt. Lett. **7**, 288 (1982).
15. T. Uesugi, B.-S. Song, T. Asano, and S. Noda, Opt. Express **14**, 377 (2006).
16. T. Tanabe, M. Notomi, S. Mitsugi, A. Shinya, and E. Kuramochi, Opt. Lett. **30**, 2575 (2005).